

Development of Cs-Free Negative-Ion Source by Sheet Plasma^{*)}

Keito HANAI, Toshikio TAKIMOTO, Hiroki KAMINAGA, Akira TONEGAWA,
Kohnosuke SATO¹⁾ and Kazutaka KAWAMURA

Tokai University, 4-1-1 Kitakaname, Hiratsuka, Kanagawa 259-1292, Japan

¹⁾*Tokyo University of Science, 1-3 Kagurazaka, Shinjuku-ku, Tokyo 162-8601, Japan*

(Received 7 January 2020 / Accepted 17 March 2020)

The use of cesium leads complicates ion source operation and requires regular maintenance for continuous operation. The development of a negative-ion source without Cs seeding is desired in neutral beam injectors. A magnetized-sheet plasma producing negative ions using volume production without Cs seeding was designed. The experiment was performed by a TPDsheet-U and tested using steady-state hydrogen plasma. Two different types of grid structures were used in the experiment to extract the negative-ion beam: single- and multi-aperture grids. The multi-aperture grids have been developed to achieve more beam current. The negative hydrogen ions were successfully extracted from the sheet plasma using both single- and multi-aperture grids. The current densities of the ion beams increased with increasing discharge current and extraction voltage. At an extraction voltage of 9.5 kV and a discharge current of 80 A, the approximate current density of the negative hydrogen ion beam was 8.4 mA/cm² for the case of single-aperture grids. At an extraction voltage of 9.5 kV and a discharge current of 50 A, the approximate current density of the negative hydrogen ion beam was 23 mA for the case of multi-aperture grids.

© 2020 The Japan Society of Plasma Science and Nuclear Fusion Research

Keywords: neutral beam heating, negative-ion source, volume production, Cs-free, sheet plasma, TPD-type plasma source

DOI: 10.1585/pfr.15.2401029

1. Introduction

Neutral Beam Injection (NBI) is an effective heating system used in International Thermonuclear Experimental Reactors (ITER). Negative-ion sources play an essential role in NBI systems that use steady-state magnetic nuclear fusion. At the ITER in Provence, France, a negative deuterium ion source has to deliver a stable extracted current of 57 A for 3600 s in deuterium and 66 A for 1000 s in hydrogen at a source pressure of 0.3 Pa (corresponding to current densities of 28.5 mA/cm² and 33.0 mA/cm², respectively), and the ratio of the co-extracted electrons to the extracted ions must be kept below unity [1–3]. Negative-ion source development for ITER NBI systems is driven and iteratively adjusted from the prototype source (BATMAN) via the half-size ITER source (ELISE) to the ITER sources (SPIDER) [4–7]. The application of cesium reduced the plasma grid surface work function, and the negative ions are formed by converting impinging atomic and ionic particles. Thus, cesium is useful for efficient negative-ion formation. Most of the negative-ion sources, including ELISE and BATMAN, used in fusion devices operate using the surface production applied cesium to increase negative-ion current. However, cesium adsorption and distribution are complex processes, and most negative-ion sources require regular maintenance for continuous operation [8]. Conse-

quently, it is beneficial to explore alternatives that would either reduce the amount of cesium consumed or not require its use at all. Thus, we are strongly motivated to develop a Cs-free negative-ion source.

Sheet plasma is one example of a Cs-free ion source. Uramoto demonstrated that H⁻ ions are efficiently produced in a thin plasma sheet [9,10]. However, the optimum H⁻ current density in a mixed hydrogen-argon plasma is only 0.309 mA/cm², which is far below the high H⁻ current density achieved by pure volume production in hydrogen infused with argon gas.

We developed a magnetized-sheet plasma produced by a Test plasma Produced by Direct current for Sheet plasma Upgrade (TPDsheet-U) to produce and control negative hydrogen ions in plasma [11–13]. In the central region of the magnetized-sheet plasma, the electron temperature is approximately 10–15 eV; however, only 1 eV at the periphery. As the high- and low-energy electron regions are narrowly spaced (by 10–20 mm), the magnetized-sheet plasma is suitable for generating negative hydrogen ions [14]. Due to the minimal plasma thickness, the geometry of the magnetized-sheet plasma crossed with that of the vertical gas flow is nearly one-dimensional, ensuring that the H⁻ ions can be quantitatively analyzed in this system.

This study is a work in progress toward realizing a Cs-free negative-ion source. The development of Cs-free negative-ion source was conducted on TPD-Sheet IV using single-aperture grids [15]. In this study, we devel-

author's e-mail: 8bsnm008@mail.u-tokai.ac.jp

^{*)} This article is based on the presentation at the 28th International Toki Conference on Plasma and Fusion Research (ITC28).

oped multi-aperture grids to achieve more beam current from the sheet plasma. Last year, the plasma source was inherited and upgraded from TPD-sheet IV to TPDsheet-U because of the extended size of multi-aperture grids. The developed ion source has a larger extraction system and enables the negative ions to be extracted from a larger area of the sheet plasma. The extraction grids were moved closer to the plasma source by about 0.3 m. The new design is expected to increase the negative-ion current. The negative-ion density ($n_{\bar{H}}$) was previously measured using an Omegatron mass spectrometer [16], and the hydrogen/deuterium negative-ion beam was also measured using single-aperture grids on TPD-Sheet IV (before the upgrade) [17, 18]. The present experiment was conducted on TPDsheet-U for both single- and multi-aperture grids. In section 2 “Experimental Setup,” we describe the Cs-free negative-ion source TPDsheet-U and basic design of multi-

aperture grids. In section 3 “Result and Discussion,” we introduce the characteristics of the developed extraction system and single-aperture grids on TPDsheet-U.

2. Experimental Setup

Our entire experimental setup is simply the linear plasma device TPDsheet-U shown in Fig. 1 (a) [18, 19]. The plasma is divided into two regions: the sheet plasma source region and the experimental region. Hydrogen plasma is produced by a modified TPD-type discharge between an LaB₆ hot cathode and a hollow anode. The cathode is composed of a tungsten filament, tungsten needle, and a fragment of LaB₆. The anode slit is 2 mm thick and 40 mm wide. The thermionic emission of LaB₆ generates an arc discharge plasma. The generated plasma is compressed into a sheet by passing it through the slits of the floating electrodes and the anode (see Fig. 1 (b)). The sheet plasma is led to the experimental region under the stationary magnetic field generated via 7 rectangular coils and terminated by an electrically floating, water-target plate axially positioned at 0.5 m (along the Z-axis) from the discharge anode. The plasma is generated under a hydrogen gas flow of 75 sccm. The discharge current is varied from 30 to 100 A. The discharge power has a maximum value of 12 kW.

The extraction system is set at the downstream of the sheet plasma region. The pumping systems are connected to both ends of the chamber in the experimental region. The gas pressure in the extraction system is held below 0.3 Pa. The rectangular magnetic coils create a uniform magnetic field in the extraction system. In the extraction region, the production and extraction of negative ions are conducted. Figure 1 (c) shows a schematic diagram of the extraction system. The chamber of the extraction system is mainly made of SUS304. Two different types of grid structures are used to extract the negative-ion beam: single-aperture grids and multi-aperture grids. The multi-aperture grids are designed to get more beam current from the sheet

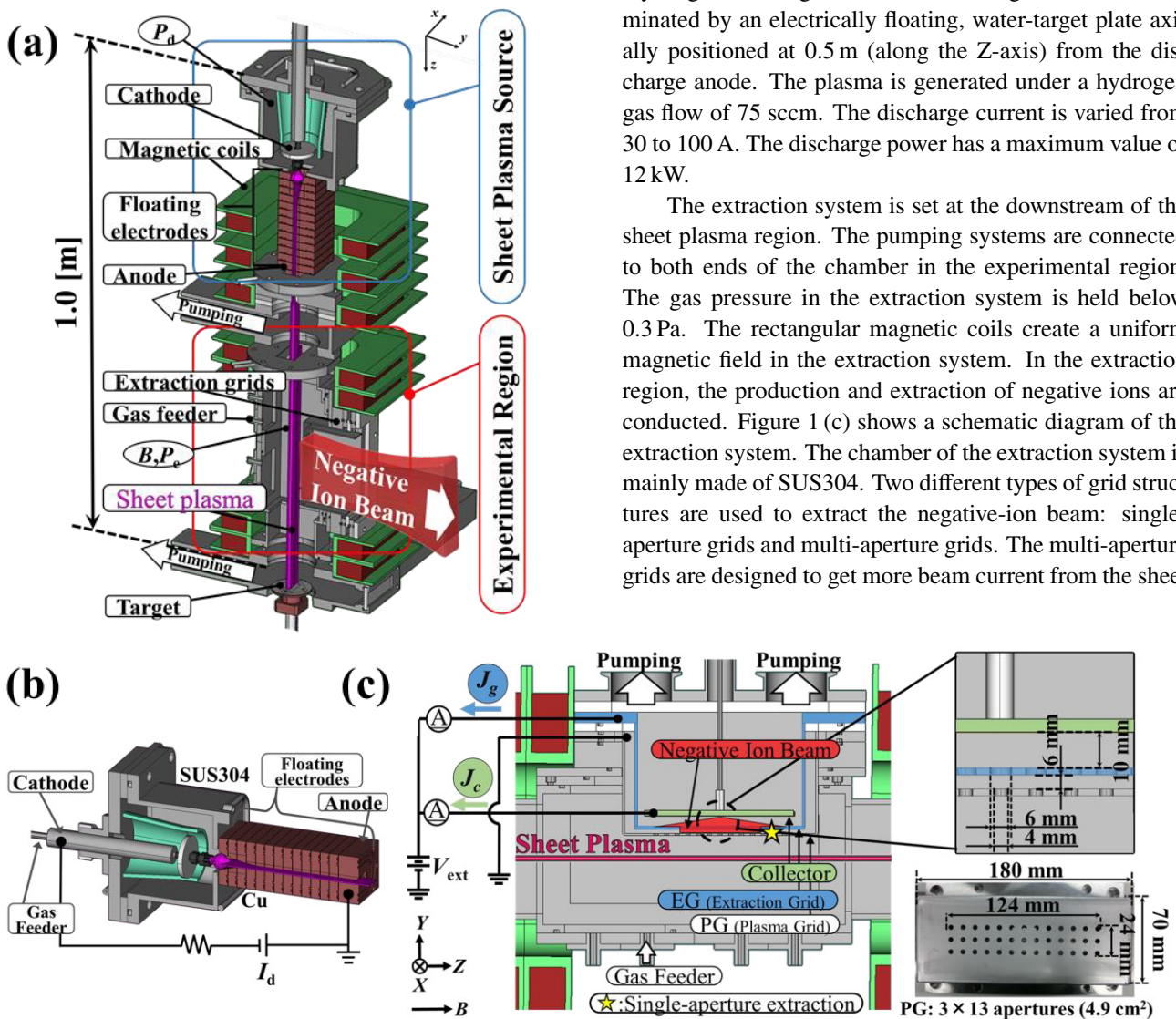


Fig. 1 (a) Schematic of the experimental setup of TPDsheet-U. (b) Schematic diagram of a TPD plasma source. (c) Schematic diagram of the extraction system.

plasma. The negative hydrogen ion beam is extracted by a two-grid extraction system located at the periphery of the sheet plasma as shown in Fig. 1 (c). The first (plasma-facing) and second grids are called the plasma grid (PG) and the extraction grid (EG), respectively. PG is approximately 180 mm high \times 70 mm in size, and EG is approximately 160 mm high \times 60 mm in size in multi-aperture grids. Each grid features 39 apertures, and each beamlet group is made of apertures arranged in a 13×3 grid. For single-aperture grids, PG has 4-mm aperture, EG has 8-mm aperture, and the gap between the grids is 6 mm. For the multi-aperture grids, PG has 4-mm aperture, EG has 6-mm aperture, and the gap between grids is 6 mm.

PG is grounded and has the same voltage as the remainder of the TPDsheet-U. A maximum voltage of approximately 10 kV is applied between PG and EG, so that in the vicinity of the PG apertures the electric field extracts the negative ions from the periphery of the sheet plasma toward the collector. Since the extraction direction is perpendicular to the magnetic field, the extracted ion beam is deflected by a magnetic force. For a field strength of 40 mT and an extraction voltage of 10 kV, our calculations show that the Larmor radius is 36 cm for fully accelerated H^- ions. The extracted ion beam hits the collector placed at a position within the Larmor radius. The extracted current densities J_c and J_g are measured at the collector and EG, respectively.

3. Results and Discussion

Figure 2 shows that the extracted current density increases linearly with the input extraction voltage, V_{ext} , for the case of single-aperture grids. For single-aperture grids, J_c and J_g are measured in the peripheral region at a distance of 24 mm from the center of the sheet plasma. The discharge current, I_d , hydrogen gas pressure and magnetic field strength, B , are 80 A, 0.3 Pa and 40 mT, respectively. B had already been optimized for extracted negative-ion current density, J , in a previous experiment [19]. At an extraction voltage of 9.5 kV, the approximate H^- current density is 8.4 mA/cm². Figure 2 shows that the extracted ion current density, J_c , still increases with V_{ext} , and the saturation of J_c and J_g is not observed.

Figure 3 shows a plot of the extracted current density, J , versus the discharge current at an extraction voltage of 9.5 kV for the case of single-aperture grids. The gas pressure is fixed at 0.3 Pa, and the magnetic field strength is 40 mT. J_c and J_g linearly increase with the discharge current. This result confirms that the extracted ion current density can be increased by increasing the discharge current. The ratio of the inevitably co-extracted electrons to the negative ions needs to remain below unity. The extracted current density is 3-7 times larger than the extracted ion current density. Currently, we are working on a way to prevent the impinging of electrons onto the grids by installing a tiny fence near the extraction aperture on PG.

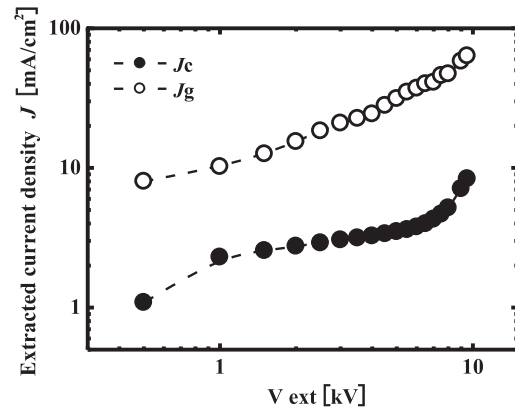


Fig. 2 The extracted current density, J , as a function of the extraction voltage, V_{ext} , in the peripheral region at a distance of 24 mm from the center of the sheet plasma for the case of single-aperture grids.

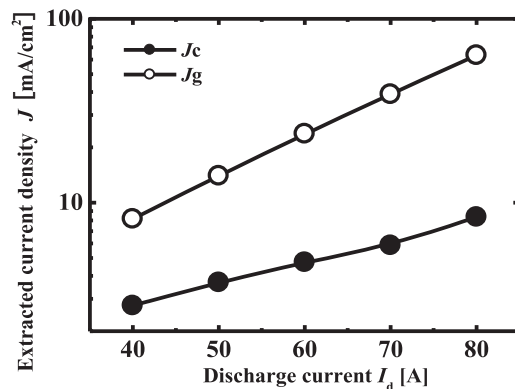


Fig. 3 The dependence of the extracted current densities on the discharge current, I_d , for an extraction voltage of 9.5 kV for the case of single-aperture grids.

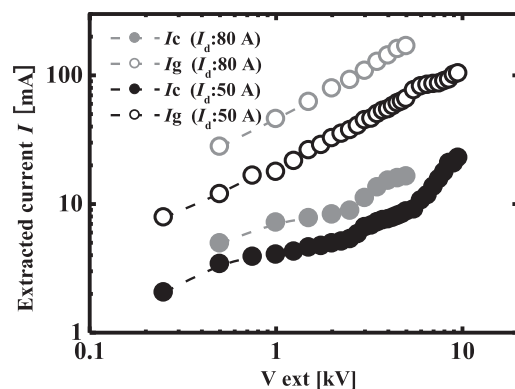


Fig. 4 The extracted current, I , as a function of the extraction voltage, V_{ext} , for the case of multi-aperture grids.

The multi-aperture grids have been optimized for negative-ion beam current from the sheet plasma. The extraction experiment is conducted via a developed device. Figure 4 shows a plot of the extracted current, I , for multi-aperture grids versus the extraction voltage. The gas pressure is 0.3 Pa, and the magnetic field strength, B ,

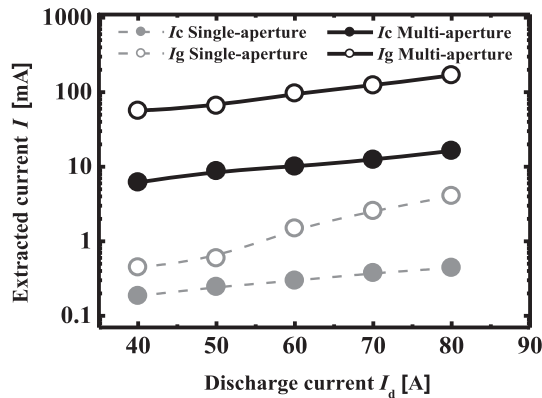


Fig. 5 The dependence of the extracted current, I , on the discharge current, I_d , for an extraction voltage, V_{ext} , of 5 kV for the case of multi-aperture grids.

is 40 mT. The negative hydrogen ions are successfully extracted from the sheet plasma. The extracted current, I_c , increases with the extraction voltage. The negative-ion beam current is obtained by multiplying the current density by the extraction area (4.9 cm^2 , 39 apertures). At an extraction voltage of 9.5 kV and discharge current of 50 A, the approximate H^- current is 23 mA (Corresponding extracted current density is 4.7 mA/cm^2). The behavior of the extraction voltage is in good agreement with that for single-aperture grids as shown in Fig. 2.

Figure 5 shows a plot of the extracted current, I , versus the discharge current at an extraction voltage of 5 kV for the case of multi-aperture grids. The gas pressure is 0.3 Pa, and the magnetic field strength is 40 mT. The extracted currents I_c and I_g are linear functions of the discharge current and therefore can be increased by increasing the discharge current. I_g is 7–10 times larger than I_c . The dependence on discharge current for multi-aperture grids is in good agreement with that for the single-aperture grids. The gray colored plot in Fig. 5 shows the results for single-aperture grids. The extracted current, I_c , for multi-aperture grids is 36 times larger than that for single-aperture grids. The multi-aperture grids have 39 ($\phi 4 \text{ mm}$, 3×13) holes to extract negative ions; thus, I_c is directly proportional to the number of apertures.

To reach ITER's requirement, the negative-ion current density, J_c , and the current, I_c , need to increase. Methods used to increase J_c include: increasing the discharge current to generate high negative ions, increasing the extraction voltage, and reducing the gap between the extraction grids because according to Child's law, J_c is inversely proportional to the gap between grids. Using any of the methods will also increase I_c since it increases with J_c . Increasing the extraction area will also help. This is why the geometry of the extraction grid will be changed from that of a circle to that of a slit.

4. Conclusions

A Cs-free negative-ion source is designed using

TPDSheet-U. The experiment is conducted using both single- and multi-aperture grids. This paper shows the basic design of multi-aperture grids and clarifies the basic characteristics of the developed system. The results are summarized below.

1. The negative hydrogen ions in the sheet plasma are successfully extracted onto the single/multi-aperture extraction grids.
2. The extracted ion current density, J_c , increases with increasing discharge current, I_d , and extraction voltage, V_{ext} . At an extraction voltage of 9.5 kV and a discharge current of 80 A, the current density, J_c , of the negative hydrogen ion beam is approximately 8.4 mA/cm^2 .
3. The extracted ion current, I_c , increases with increasing discharge current, I_d , and extraction voltage, V_{ext} . At an extraction voltage of 9.5 kV and a discharge current of 50 A, the extracted ion current, I_c , of the negative hydrogen ion beam is approximately 23 mA.

Acknowledgments

This study had been supported by the LHD Joint Project of the National Institute for Fusion Science (NIFS16KOAR021).

- [1] U. Fantz *et al.*, Nucl. Fusion **49**, 125007 (2009).
- [2] U. Fantz *et al.*, Nucl. Fusion **57**, 116007 (2017).
- [3] U. Fantz *et al.*, Chem. Phys. **398**, 7 (2012).
- [4] B. Heinemann *et al.*, AIP Conf. Proc. **1655**, 060003 (2015).
- [5] B. Heinemann, D. Wunderlich, W. Kraus, F. Bonomo, U. Fantz, M. Fröschele, I. Mario, R. Riedl and C. Wimmer, Fusion Eng. Des. **146**, 455 (2019).
- [6] D. Wunderlich *et al.*, Nucl. Fusion **59**, 084001 (2019).
- [7] P. Agostinetti *et al.*, Nucl. Fusion **56**, 016015 (2016).
- [8] U. Kurutz *et al.*, Plasma Phys. Control. Fusion **59**, 075008 (2017).
- [9] J. Uramoto, AIP Conf. Proc. **158**, 319 (1987).
- [10] V.R. Noguera, G.Q. Blantocas and H.J. Ramos, Nucl. Instrum. Methods **B 266**, 2627 (2008).
- [11] M. Otsuka, K. Tkayama, A. Tanaka, J. Uramoto, S. Aihara, T. Kodama, K. Ishii and Y. Tanaka, Proceedings of the 7th International Conference on Phenomena in Ionized Gases, 420-423 (1966).
- [12] K. Sunako, K. Nanri, E. Yabe and K. Takayama, Nucl. Instrum. Methods, Phys. Res. Section B **111**, 151 (1996).
- [13] A. Tonegawa, M. Ono, Y. Morihira, H. Ogawa, T. Shibuya, K. Kawamura and K. Takayama, J. Nucl. Mater. **313-316**, 1046 (2003).
- [14] R. Endo, S. Ishihara, T. Takimoto, A. Tonegawa, K. Sato and K. Kawamura, AIP Conf. Proc. 020009 (2018).
- [15] S. Ishihara, T. Takimoto, R. Endo, A. Tonegawa, K. Sato and K. Kawamura, AIP Conf. Proc. 050015 (2018).
- [16] A. Tonegawa, K. Kumita, M. Ono, T. Shibuya and K. Kawamura, Jpn. J. Appl. Phys. **45**, 8212 (2006).
- [17] T. Iijima, S. Hagiwara, S. Tanaka, A. Tonegawa, K. Kawamura and K. Sato, Fusion Sci. Technol. **63**, 417 (2013).
- [18] T. Iijima, H. Kobayashi, S. Tanaka, A. Tonegawa, K. Kawamura and K. Sato, Plasma Fusion Res. **9**, 2405010 (2014).
- [19] K. Hanai, S. Ishihara, R. Endo, T. Takimoto, A. Tonegawa and K. Sato, Fusion Eng. Des. **146**, 2721 (2019).